Heat and Mass Transfer (2021) 57:853–872
https://doi.org/10.1007/s00231-020-02999-3

ORIGINAL

Drying kinetics of tomato (*Solanum lycopersicum*) and Brinjal (*Solanum melongena*) using an indirect type solar dryer and performance parameters of dryer

Abhay Lingayat[1] · Chandramohan V. P.[1] · Raju V. R. K.[1] · Suresh S.[2]

Received: 9 May 2019 / Accepted: 7 November 2020 / Published online: 13 November 2020

Abstract

Tomato (*Solanum lycopersicum*) and brinjal (*Solanum melongena*) are food products that are frequently wasted in Indian markets as their shelf lives are only a few days. An indirect type solar dryer (ITSD) has been developed. It's performance and drying kinetics of brinjal and tomato slices have been analyzed. The moisture content of tomato decreased from 15.667 to 0.803 kg/kg of dry basis (db) and that of brinjal reduced from 10.111 to 0.498 kg/kg of db. The drying curve was fitted with the different models of existing studies. The average effective moisture diffusivity is estimated and it is 3.60×10^{-9} and 4.00×10^{-9} m^2/s for tomato and brinjal, respectively. Mass transfer coefficient was in the range of 0.82×10^{-4} to 2.85×10^{-3} m/s for tomato and 1.11×10^{-4} to 3.32×10^{-3} m/s for brinjal. The heat transfer coefficient was in the range of 0.089 to 2.888 W/m^2 K and 0.1066 to 3.3564 W/m^2 K for tomato and brinjal, respectively. The activation energy for tomato and brinjal was 21.19 and 19.46 kJ/mol, respectively. The average thermal efficiency of the collector and dryer was 59.05% and 31.4% during tomato drying and 58.42% and 25.16% for brinjal drying, respectively.

Keywords Indirect type solar dryer · Solar air collector · Thermal efficiency · Drying efficiency · Heat and mass transfer coefficients · Diffusion coefficient

Nomenclature

a, b	coefficients.
A	Area (m^2).
A_m	surface area of the material (m^2).
C_p	specific heat at constant pressure (kJ/kg K).
D_{AB}	moisture diffusivity of water in air (m^2/s).
D_{eff}	Effective moisture diffusivity (m^2/s).
D_o	Pre-exponential factor (m^2/s).
db	Dry basis.
E	Activation energy (kJ/mol).
h	Heat transfer coefficient, (W/m^2K).
$\boldsymbol{h_m}$	Mass transfer coefficient (m/s).
H	Latent heat (kJ/kg).
I	total solar energy (kW).
I_c	solar radiation on the collector (W/m^2).
ITSD	Indirect type solar dryer.
$\boldsymbol{k_a}$	Thermal conductivity of drying air (W/m K).
k, g	drying constants (h^{-1}).
L	Thickness of the sample material (m).
Le	Lewis number.
m	Mass (kg).
$\dot{m}_a$	mass flow rate (kg/s).
MC	moisture content (kg/kg of dry basis).
MR	moisture ratio.
N	total number of observations.
n	number of constant.
Q	heat energy (kJ).
R	Correlation coefficient.
R_g	universal gas constant (J/ mol K).
RH	Relative humidity (%).
SAC	Solar air collector.
T	Temperature (°C).
V	Volume of the material (m^3).
wb	Wet basis.

✉ Chandramohan V. P.
vpcm80@nitw.ac.in

[1] Mechanical Engineering Department, National Institute of Technology Warangal, Warangal, Telangana 506004, India

[2] Mechanical Engineering Department, National Institute of Technology Tiruchirappalli, Tiruchirappalli, Tamilnadu 620015, India

X_1, X_2, X_3, X_n Uncertainties of independent variables.
Z Uncertainty.

Greek Symbols

α thermal diffusivity (m^2/s).
η Efficiency (%).
χ reduced chi-square.

Subscripts

a air.
c collector.
d Dryer.
exp Experimental.
f final.
i Initial.
m material.
out outlet.
pre Predicted.
t Total.
w Water.

1 Introduction

Growing agricultural food products is a time-consuming process, needs a lot of manpower and need much careful protection from animals and insects. It is difficult to hear the food wastage after such type of tough and careful harvesting process. Tomato (*Solanum lycopersicum*) and brinjal or eggplant (*Solanum melongena*) are cultivated extensively for its edible fruit. Tomato and brinjal are popular vegetables all over the world because of their good nutritional value, and their taste and flavor. In India, the productions of tomato and brinjal are near about $19{,}542 \times 10^3$ and $12{,}323 \times 10^3$ metric tons per year, respectively. They are the frequent food products that are damaged / rotted because of their poor shelf life (1 to 5 days) and improper preservation [1].

Drying is a processing technique that is used to preserve the agricultural products for a long time by removing the moisture up to a safe limit. Drying is an energy consuming process and the energy needed for the drying process is mainly derived from fossil fuels which create negative impacts on the environment and its price also increasing day by day [2]. Solar energy is an effective alternative to fossil fuels and it can be used to dry food products as the drying of food is a low temperature application. Open sun drying (OSD) is a traditional method for food drying from ancient days but it has limitations such as contamination of dust, lower drying rate, losses due to animals and birds, dew factor etc. Issues related to OSD can be rectified by using an indirect type solar dryer (ITSD). ITSD has a number of advantages such as good quality products, lower drying period, dust free products and large-scale products. Also, in recent years, the performance of the drying system was improved by providing artificial roughened or corrugation absorber surface of solar air collector (SAC) [3–6].

Several studies have been noticed on the drying of agricultural fruits and vegetables. Ringeisen et al. [7] developed solar crop dryers with a solar concentrator. Tomatoes were dried from initial moisture content (MC) of 90% wet basis (wb) to the final MC of 10%. The effect of solar concentrator on the drying rate of tomatoes was studied. It was observed that the drying time was reduced to 21% compared to the dryer without concentrator. Quality analysis was carried out on dried tomato slices and found that there were no changes in quality in the dryer with and without concentrator.

Atalay [8] studied the performance, energy and exergy analysis of ITSD system with thermal energy storage of packed bed type by analyzing drying kinetics of orange slices. Results showed that MC of the sample reduced from 15.38 to 1.114 kg per kg of db. The exergy efficiency was found to be in the range from 50.18 to 66.58% during the sunshine hour and 54.71 and 68.37% using TES device. They have also developed a numerical model [9] for the drying of apple slices using solar energy.

Oberoi and Sogi [9] conducted experiments on watermelon pomace in the fluidized-bed dryer (FBD) and cabinet drying chambers. It was found that effective moisture diffusivity (D_{eff}) of pomace was in the range of 8.80×10^{-9} to 35.41×10^{-9} m^2/s for fluidized bed and 3.47×10^{-9} to 8.68×10^{-9} m^2/s for cabinet dryers. Lycopene content was observed to be 0.011–0.0173 and 0.0093–0.0154 g/100 g dry basis (db) in FBD and cabinet dryer, respectively. Similar studies were performed by Monteiro et al. [10] to estimate the influence of water activity and dehydration ratio of pumpkin slices.

Torki-Harchegani et al. [11] studied the drying behavior of the lemon slices in different temperatures of 50, 60 and 75 °C in the air-ventilated oven dryer. Slices were dried from the initial MC of 6.14 kg per kg of db to the final MC of 0.2 kg per kg of db. Midilli and Kucuk model were considered to be the best drying model for lemon slices. D_{eff} was calculated to be 1.62×10^{-11}, 3.25×10^{-11} and 8.11×10^{-11} m^2/s at 50, 60 and 75 °C, respectively. Also, the activation energy and Arrhenius constant were estimated to be 60.08 kJ/mol and 0.08511 m^2/s, respectively.

Akpinar and Bicer [12] used cyclone dryer to understand the thin-layer drying behavior of brinjal with air temperatures of 55, 65 and 75 °C at air velocities of 1 and 1.5 m/s. Brinjal was dried from an initial MC of 10.63 kg per kg of db to a final MC of 0.04 kg per kg of db. Doymaz and Gol [13] studied the effect of air temperatures (in the range of 50 to 80 °C) and slice thickness (0.5 to 1 cm) on the drying characteristics of blanched eggplant followed by drying in an electric cabinet dryer. MC content of brinjal was reduced from its initial value of 92.84% to the final value of 10% (wb). El-Sebaii and Shalaby et al. [14] developed a forced convection ITSD. Experimental analysis was carried out for the drying of

thymus and mint. Thymus was dried from an initial MC of 95% (wb) to final MC of 11% (wb) for a drying time of 5 h while mint was dried from an initial MC of 85% (wb) to final MC of 11% (wb) for a drying time of 34 h.

Dissa et al. [15] developed a solar dryer and studied Amelie and Brooks mangoes' drying characteristics. Amelie and Brooks mangoes were dried up to the final MC of 1.3303 and 2.9691 kg per kg of db. Obtained results were fitted with different available mathematical models and found that two-term model gave the best fit. The drying rate and drying efficiency were in the range of 0 to 0.15 g kg^{-1} s^{-1} and 0 and 34%, respectively. Effective diffusivity was estimated and it was from 2.7906×10^{-11} and 1.8489×10^{-10} m^2/s. A bunch of mango slices was dried in a large scale rectangular solar dryer setup by Wilkins et al. [16]. Drying curves were fitted with other models and the model correlation coefficients were found. Wang et al. [17] presented a forced convection ITSD with an auxiliary heating source for mango drying. The impact of air temperature on the performance of the system and drying behavior of mango slices were investigated.

Shrivastava and Kumar [18] developed an ITSD with corrugated double pass SAC for drying of fenugreek. It was observed that the average convective heat transfer coefficient was varied from 0.45 to 6.91 W/m^2 °C. Akpinar [19] carried out the exergy analysis on thin layer drying characteristics of long green pepper with a forced convection ITSD. It was concluded that the exergetic efficiency decreased with the increase of drying time. Tiwari and Tiwari [20] conducted experiments in a solar greenhouse dryer integrated with the semi-transparent photovoltaic module and evaluated different drying parameters such as relative humidity, drying air temperature, heat and mass transfer coefficients, etc. The convective heat transfer coefficient was in the range of 0.84–3.1 W/m^2 K. They suggested that the Page model was the best fitting model to study the drying behavior of grapes.

Arunsandeep et al. [21] carried out a numerical analysis on the drying behavior of spherical objects by considering green peas as a food material. It was reported that air temperature was one of the dominant parameters during drying. It was concluded that for achieving 10% of final MC, green peas should be dried for a minimum period of 7.448 and 3.73 h at drying temperatures of 45 °C and 75 °C, respectively. Mahapatra and Tripathy [22] performed the drying experiments on carrot slices in direct, indirect and mixed type solar dryer and determined the heat transfer coefficient during drying. They also carried out the numerical analysis and found the temperature distribution in the carrot. Numerical results were compared and found good agreement with experimental results.

Different methods have been used for the drying of fruits and vegetables such as fluidized-bed drying [9], convective drying [11–13], freeze drying [23] and solar drying [7, 17, 22]. Different agricultural foods such as tomato [7], orange slices [8], lemon slices [11], brinjal [12, 13], mango [15, 17], green pepper [19], and carrot [22] have been dried using these methods. Some numerical studies have also contributed to the drying behavior of food materials [21, 22, 24]. From the literature, it is found that none of the works discussed drying of tomato and brinjal in ITSD. Very limited data is available in the literature about the drying kinetics of tomato [7] and brinjal [12, 13]. Important drying parameters such as diffusion coefficient, heat and mass transfer coefficients and activation energy of tomato and brinjal have not been estimated. There is no study found on drying experiments in ITSD with V shape corrugated absorber plate. This work overcomes the above limitations.

The main objectives of the present work, therefore, are; (i) to develop an ITSD experimental setup with V-shape corrugation absorber plate to conduct drying experiments with tomato and brinjal, (ii) to estimate the initial MC of tomato and brinjal, (iii) to find the transient MC distribution of tomato and brinjal at different trays inside the drying cabinet, (iv) to investigate the thermal performance of ITSD and solar air collector, (v) to identify a suitable drying model for tomato and brinjal and (vi) to estimate the drying parameters such as diffusion coefficient, heat and mass transfer coefficients and activation energy of tomato and brinjal.

2 Materials and methods

2.1 Experimental setup of ITSD

An ITSD was developed at the National Institute of Technology Warangal, India (Longitude 79.58° E; Latitude: 18.0° N). Warangal's usual average solar radiation is 676.4 W/m^2 on 23.5° inclined surface toward the south [25, 26]. The developed ITSD consists of SAC with V-shaped absorber surface, drying chamber with a chimney at the top and measuring instruments for different parameters. The schematic view of ITSD is shown in Fig. 1. The drying chamber consisted of four plastic trays (net type) for keeping the food products to be dried.

The other components and accessories of ITSD are shown in Table 1. It was found from the authors' previous study [27] that an artificial roughness over the absorber plate created a heat gain of up to 106% compared to the smooth surface. Therefore, a V-shaped absorber plate was selected for this present setup to encourage the heat transfer rate between the flowing air and absorber surface. The SAC box was made from 5 mm thick galvanized iron frame. The working fluid was allowed to flow between the copper absorber plate and the collector plate. It was then allowed to flow over the V-shaped corrugation. Rock wool insulation was placed at the surface below the collector plate. Heat loss regions in the setup were identified and rectified using proper insulation materials, as

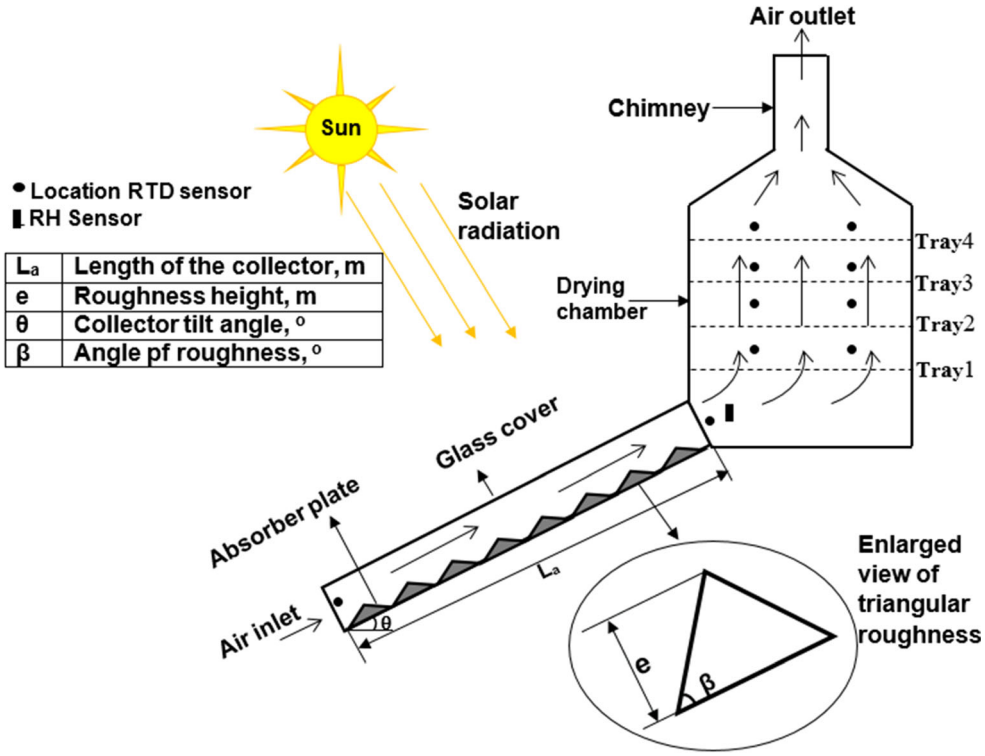

Fig. 1 Layout of indirect type solar dryer (ITSD)

drying is a low temperature application so that every possibility of heat loss in the setup ruins the system performance.

Table 2 shows different instruments and their specifications used for the measurement of different parameters. Temperatures are measured with RTD sensors on each tray. T_1, T_2, T_3, T_4, and T_{atm} are the temperature at tray - 1, 2, 3, 4, and the atmosphere, respectively. Radiation intensity, air humidity and air velocity were measured during experiments. Mass of the product was measured at each hour by a hot air oven.

2.2 Experimental procedure

The experiments were carried out with slices of tomato and brinjal. The experiments were conducted during April 2018 in NIT Warangal, India. Fresh tomato and brinjal were procured from the local market of Hanamkonda, Warangal, India. For effective drying, 4–6 mm thicknesses of tomato and brinjal slices were selected. Tomato and brinjal slices were cut into cylindrical slices as mentioned in Fig. 2. Initially, 500 g of tomato slices were spread uniformly on each tray for drying. Then all four trays were kept in the drying chamber. The doors of the cabinet were properly closed. During the experiments, different properties such as solar insolation, velocity, temperature and relative humidity at each hour were measured to analyze the dryer performance and drying characteristics of materials. MC_i of tomato and brinjal were estimated using a separate device, a hot air oven (230 V, 3500 W, 15 A). Similar

Table 1 Components and accessories of the ITSD with their specifications

Component	Specifications
Gross dimensions	2 m × 1.05 m × 0.125 m.
Absorber surface	2 m × 0.9 m of corrugated V shape with selective black colour coating.
Absorber material	1 mm Copper sheet.
Thickness of glazing	5 mm.
Glazing material	Window glass.
Collector tilt angle	30° (With horizontal).
Mode of air flow	Natural air flow.
Air flow channels	Made by rockwool and its thermal conductivity is 0.04 W/m K.
Dimensions of drying chamber	0.35 m × 0.85 m × 0.70 m.
Material for tray	Plastic mesh.

Table 2 Instruments used during experiments with specifications

Instrument	Brand and model	Range/ specification	Accuracy
RTD Pt-100 sensor	PPI Make- India	0–400 °C	±1 °C
16 channels data logger	PPI Make- India	–	± 0.25%
Solar power meter	Tenmar TM 207- Taiwan	0–2000 W/m^2	± 10 W/-m^2
Hot wire anemometer	Tenmar, Model: TM 4002	−20 to 80 °C,	±1 °C
		0 to 80% RH	±3% RH
		0 to 20 m/s,	± 0.03 m/s
Humidity transmitter	Make: PPI- Taiwan, Model: RH-33,	Temperature: −40 to 85 °C	±1 °C
		RH: 0–100%	± 2% RH
Weighing balance (Electronic)	Model: OHAUS PA 214, make: USA	0–200 g	± 0.2 mg
Hot air oven	PPI Make- India	230 V, 3500 W, 15 A,	–
	Model BTI 30	Temperature: 0–250 °C	

procedures and measurements were followed during the drying experiments for brinjal.

2.3 Performance analysis parameters

2.3.1 The total heat required for the drying process

SAC of ITSD converts solar radiation from the sun into useful heat which is used to eliminate MC from the material to be dried. The amount of heat required to evaporate MC from the material includes energy for initial heating of the material and evaporation of water.

Quantity of heat needed for heating the material to be dried,

$$Q_m = C_{pm} m_i \left(T_{mf} - T_{mi}\right), \tag{1}$$

where C_{pm} is the specific heat of material (kJ/kg K), subscripts, i is initial and f is final.

Quantity of heat required for evaporation of moisture from the material is:

$$Q_e = H\left(m_i - m_f\right), \tag{2}$$

Where, H is the latent heat of vaporization (kJ/kg).

Total heat required for drying operation is,

$$Q_t = Q_m + Q_e, \tag{3}$$

Fig. 2 shape of sample

2.3.2 Heat available from SAC

The amount of heat given by SAC (or) heat available for drying can be expressed as,

$$Q_a = \dot{m}_a C_{pa}(T_{cout} - T_i), \tag{4}$$

Here, subscript a represents air and *cout* is the outlet of SAC.

The efficiency of SAC can be influenced by many factors like geographical location, ambient air velocity, temperature, humidity etc. The efficiency of SAC can be calculated as,

$$\eta_c = \frac{Q_a}{I} = \frac{\dot{m}_a C_{pa}(T_{cout} - T_i)}{A_c I_c,} \tag{5}$$

Where, A_c is the area of collector, I_c is solar intensity falling on the collector (W/m^2).

The solar fraction (SF) is estimated with the help of energy supplied by SAC (Q_a) and energy needed to eliminate MC from the product (Q_t).

$$SF = \frac{Q_a}{Q_t}, \tag{6}$$

2.4 Drying characteristics of tomato and brinjal slices

Initial MC in wet basis (wb) and dry basis (db) is estimated using the following equations,

$$MC_i = \frac{m_i - m_d}{m_i}, \tag{7a}$$

$$MC_i = \frac{m_i - m_d}{m_d}, \tag{7b}$$

Where, m_i *and* m_d are initial and completely dried mass of the product, respectively.

Initial MC content is estimated using a hot air oven method. Tomato and brinjal slices were dried in an oven with continuous heating of 24 h and the temperature was maintained at 105 °C as per ASTM standards [28, 29]. Different experiments were conducted with different pieces and finally, an average was estimated to get the initial MC value. The average initial MC of tomato is 15.6667 kg/kg of db (mean deviation of 0.051 kg/kg of db) and that of brinjal is 10.1976 kg/kg of db (mean deviation 0.427 kg/kg of db). These are, 0.94 kg/kg of wb (for tomato) and 0.91 kg/kg of wb (for brinjal). It was reported that initial MC of tomato was 17.164 kg/kg of db in the study by Doymaz [30] and that of brinjal is 10.63 kg/kg of db in the study by Akpinar and Bicer [12] as these values slightly vary depending on regional and climatic factors.

The drying rate (DR) of the material in ITSD is estimated using MC at two successive times divided by the difference in time (*dt*) and this is calculated as follows:

$$DR = \frac{dMC}{dt} = \frac{MC_{t+dt} - MC_t}{dt}, \tag{8}$$

The drying efficiency (η_d) of ITSD is estimated using,

$$\eta_d = \frac{(m_i - m_f)\left[\gamma + C_{pw}(T_{do} - T_a)\right]}{Q_a} \times 100\%, \tag{9}$$

Subscripts, *w* mentions water, *do* is the outlet of the drying chamber.

The experimental data of moisture ratio (MR) for drying of tomato and brinjal is used to find the drying model available in the literature. MR can be expressed as,

$$MR\ (db) = \frac{MC_t - MC_e}{MC_i - MC_e}, \tag{10}$$

where, MC_t is moisture content (db) at a particular instant of time, MC_e is equilibrium MC (db) of the sample. Due to continuous variation in temperature and RH value inside the chamber during the experiments, Eq. (10) is simplified [31] as

$$MR\ (db) = \frac{MC_t}{MC_i}, \tag{11}$$

2.4.1 Available models from the literature

The drying kinetics and MC in the material at a particular instant of time can be predicted by several empirical correlations available [14, 32] in the literature. For the present study, some thin-layer models as mentioned in Table 3 were used to get the best fitting curve.

To obtain a good drying model, a non-linear regression analysis has been carried out using OriginPro 2018.

Table 3 Empirical correlations for the thin-layer drying

Model name	Expression
Lewis or Newton [31]	$MR = \exp(-kt)$,
Page model [31]	$MR = \exp(-kt^n)$,
Henderson and Pabis [31]	$MR = a\ \exp(-kt)$,
Wang and Singh [31]	$MR = 1 + at + bt^2$,
Two-term [31]	$MR = a\ exp\ (-kt) + b\ exp\ (-gt)$.

$$R^2 = 1 - \frac{\sum_{i=1}^{N}\left(MR_{pre,i} - MR_{exp,i}\right)^2}{\sum_{i=1}^{N}\left(MR_{exp,i}\right)^2}, \tag{12}$$

$$\chi^2 = 1 - \frac{\sum_{i=1}^{N}\left(MR_{pre,i} - MR_{exp,i}\right)^2}{N - n}, \tag{13}$$

Where, R^2 is the correlation coefficient, χ^2 is the reduced chi-square, subscripts *exp* and *pre* mention the experimental and predicted results, *N* is the total number of observations, and *n* is the number of constants. Levenberg-Marquardt method is used for curve fitting and finding $R^2$and χ^2. The goodness of the fit is expressed by the highest value of R^2 and lowest value of χ^2.

2.4.2 Effective moisture diffusivity

The water diffusivity of the biological material is generally evaluated with the help of simplified Fick's second law, which is called as Fick's diffusion Eqs. [17] and expressed as,

$$\frac{\partial MR}{\partial t} = D_{eff}\nabla^2 MR\ , \tag{14}$$

Tomato and brinjal were cut into cylindrical slices as shown in Fig. 2. The diffusion takes place through the thickness of slices and therefore, the solution of the slab is enough to predict the MC inside the product. Simplified analytical solution of the above partial differential equation has been proposed by Crank for different solid geometries and a slab is written as [11, 30, 33] by assuming negligible shrinkage, uniform thickness and uniform initial moisture distribution and it is expressed as

$$MR = \frac{8}{\pi^2}\sum_{i=0}^{\infty}\frac{1}{(2i+1)^2}\,exp\left[-\frac{(2i+1)^2\pi^2 D_{eff}\,t}{4L^2}\right], \tag{15a}$$

Where, L is the thickness of the slice, D_{eff} is effective moisture diffusivity.

After truncating the higher terms of the series, Eq. (15) may be expressed as:

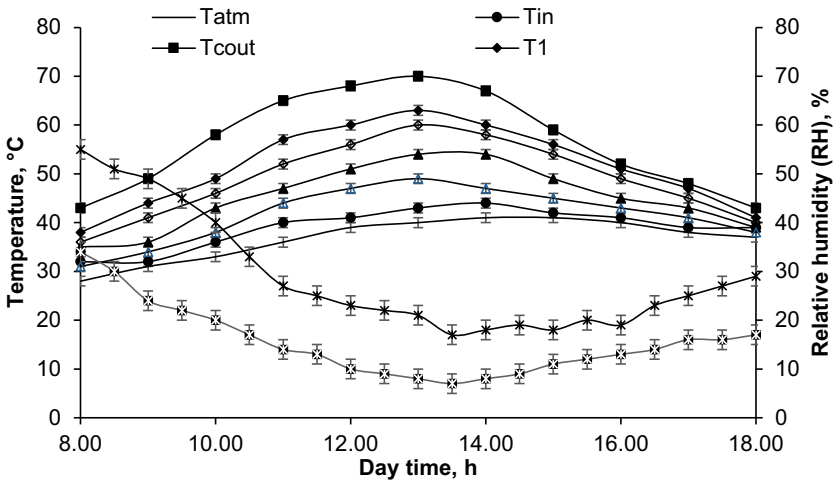

Fig. 3 Variation of temperature and relative humidity with time at different places during drying of tomato

$$MR = \frac{8}{\pi^2} exp\left[-\frac{\pi^2 D_{eff}\, t}{4L^2}\right], \tag{15b}$$

Temperature and diffusivity are related by the Arrhenius equation and are used to estimate the activation energy (E).

$$D_{eff} = D_o exp\left(\frac{-E}{R_g\,(T + 273.15)}\right), \tag{16}$$

Where D_o is the pre-exponential factor.

2.4.3 Heat and mass transfer coefficients (h and h_m)

h and h_m are surface properties of the materials which need to be estimated as they give a good understanding of drying physics. h_m in the material in terms of MR which can be estimated [34] using;

$$h_m = \frac{V}{A_m t} \ln(MR), \tag{17}$$

Where V is the volume of the material, A_m is the surface area of the material.

The shapes of the tomato and brinjal slices are cylindrical (as used in experiments). Then h_m can be estimated using Eq. (17) for both tomato and brinjal, respectively.

h and h_m can be written using the relation between thermal and concentration boundary layer [35] and from that h is estimated using,

$$h = h_m\left(\frac{k_a}{D_{AB} Le^{1/3}}\right), \tag{18}$$

where, k_a thermal conductivity of air, D_{AB} is moisture diffusivity of water in the air (0.282×10^{-4} m^2/s [36]), Le is Lewis number which represents the relative measure of thermal as well as concentration boundary layer thickness and it is calculated using:

$$L_e = \frac{\alpha_a}{D_{AB}}, \tag{19}$$

Where, α_a is the thermal diffusivity of drying air.

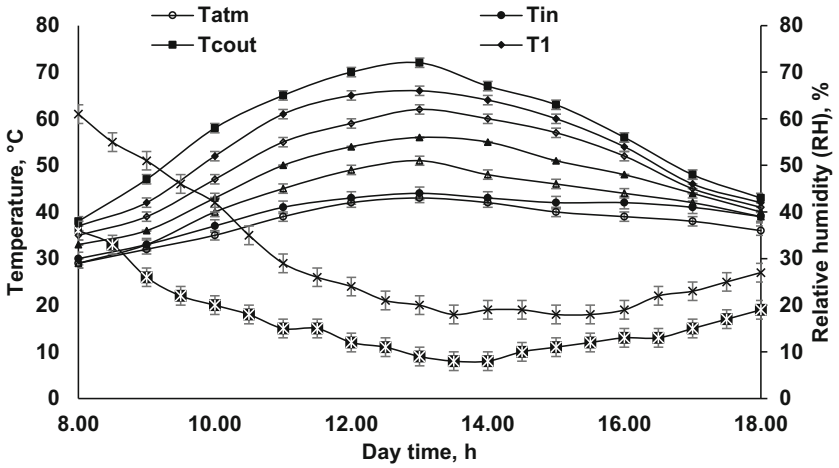

Fig. 4 Variation of temperature and relative humidity with time at different locations during drying of brinjal

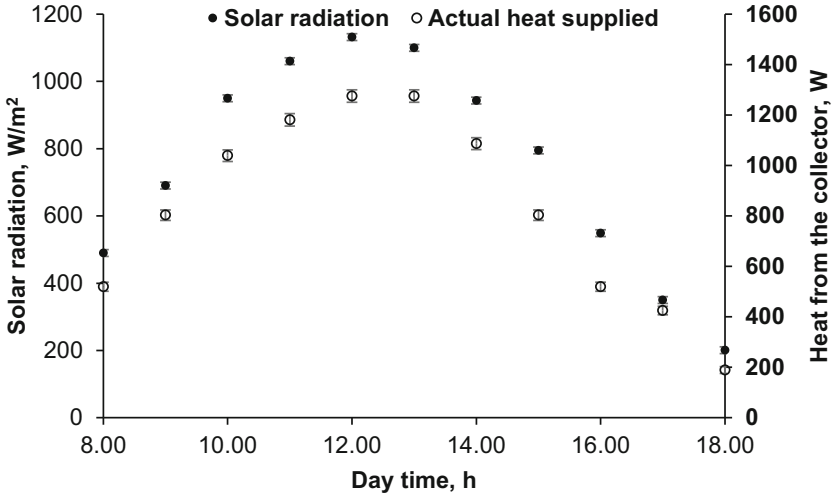

Fig. 5 Variations of instantaneous solar radiation and heat supplied during drying of tomato slices

3 Results and discussion

3.1 Performance of solar dryer

Air temperature is an important parameter that affects the drying behavior of the material. Figs. 3 and 4 show the variation of temperature with time at various locations inside the chamber during the drying of tomato and brinjal, respectively. The following notations were used for the measured temperatures during experiments. They are;

The temperature at open atmospheric air T_{atm}.

The temperature at the inlet of SAC T_{in}.

The temperature at the outlet of SAC (or inlet of drying chamber) T_{cout}.

The temperatures at trays – 1, 2, 3 and 4 T_1, T_2, T_3 and T_4.

It is noticed from Figs. 3 and 4 that the temperature of the air decreases gradually when air flows through the trays - 1, 2, 3 and 4 as each tray consists of food materials and they absorb the heat energy and eliminate moisture. In Fig. 3 (during drying of tomato) the temperature inside the chamber is minimum for the upper tray – 4 (T_4) and maximum for lower tray – 1 (T_1). Among the transient temperature distribution during tomato drying at tray - 1, T_1 reached its maximum (63 °C) at 1.00 PM. Similarly, the other maximum values of tray – 2, 3 and 4 (T_2, T_3 and T_4) were 60, 54 and 49 °C. The average temperature for T_{cout}, T_1, T_2, T_3, T_4 and T_{atm} were observed as 56.45, 51.45, 48.82, 45.09, 42.54 and 36.72 °C, respectively (Fig. 3). Also, during these experiments, the maximum temperature noticed inside the chamber was 70 °C and it was achieved at the outlet of SAC at 1.00 PM.

The maximum temperatures achieved at 1.00 PM during drying of brinjal (Fig. 4) were T_{cout}, T_1, T_2, T_3, T_4, T_{in} and T_{atm} were 72, 66, 62, 56, 51, 45 and 43 °C, respectively. The average temperature was estimated at each location (as mentioned above) from 8.00 AM to 6.00 PM and they were; 57.45, 53.72, 50.36, 46.54, 42.36, 39.72, 37.72 °C, respectively.

Figures 3 and 4 also show the variation of relative humidity (RH) during the drying of tomato and brinjal, respectively. It was noticed that RH of air at the drying cabinet inlet was less

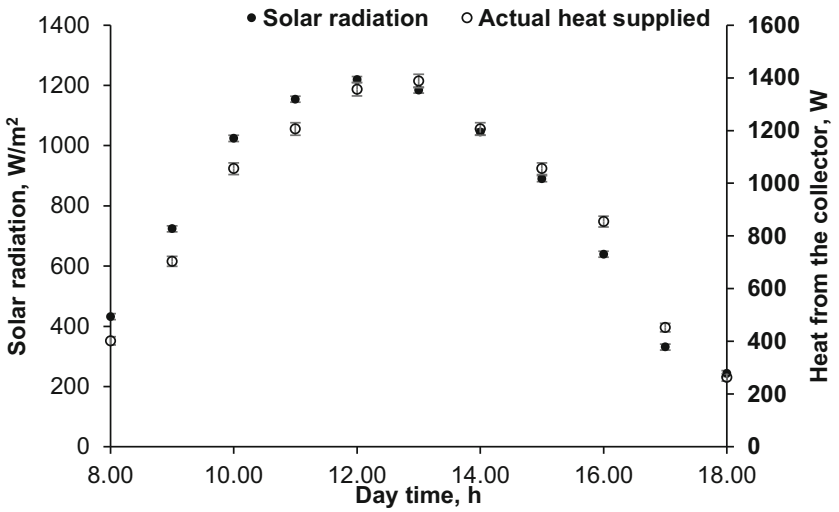

Fig. 6 Variations of instantaneous solar radiation and heat supplied during brinjal drying

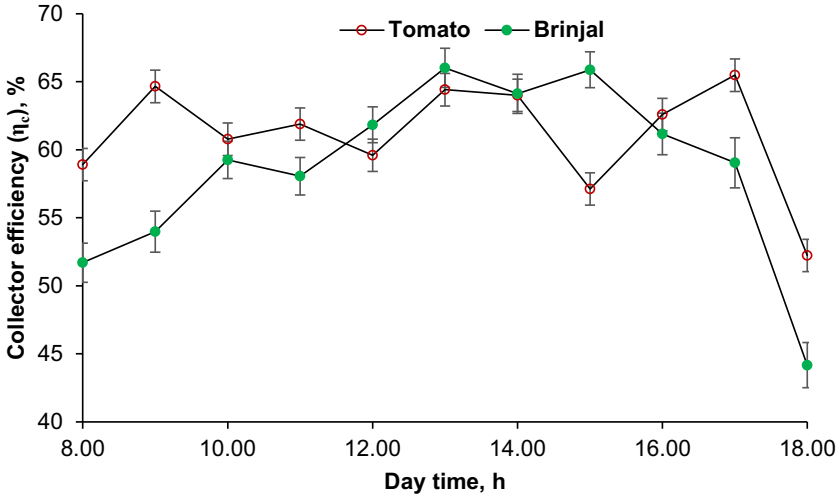

Fig. 7 Variations in thermal efficiency (η_c) of the solar air collector with time

than ambient which is useful for enhancement of drying rate as low humid air can absorb more moisture from the material. The average RH of atmospheric air and drying chamber inlet was 28.85% and 15.95% during tomato drying and it was 29.43% and 16.81% during brinjal drying, respectively.

Instantaneous solar radiation (I_c) was measured during tomato drying experiments and is shown in Fig. 5. The measurements were taken from 8.00 AM to 6.00 PM. The measured values varied from 490 W/m^2 (8.00 AM) to reach a maximum (1132 W/m^2) at noon and a minimum of 201 W/m^2 at 6.00 PM with an average of 753.14 W/m^2. Heat available for the drying system (Q_a) which is estimated using Eq. (4) is also plotted in Fig. 5. It is the function of T_{cout} and m_a. Q_a varied from 188.94 W (at 6.00 PM) to 1275.34 W (at 1.00 PM) with an average value of 824.46 W. Both variations (I_c and Q_a) are interrelated because higher I_c gives higher T_{cout} as the SAC heats the air. Therefore, as Q_a increases, the variation is almost proportional to each other (Fig. 5).

A similar measurement is performed for the drying of brinjal and the results are shown in Fig. 6. Maximum I_c was noticed at noon 1219 W/m^2 and the minimum was 243 W/m^2. Q_a varies from 263.14 to 1387.74 W.

Collector efficiency (η_c) is estimated using Eq. (5) and mentioned in Fig. 7. The fluctuation in the efficiency curve is due to continuous variation in solar radiation throughout the day. η_c varied with a minimum value of 52.2% and a maximum of 65.5% during tomato drying. A minimum of 44.2% and a maximum of 66.02% were noticed during the brinjal drying operation. Drying efficiency (η_d) is calculated (using Eq. 9) and mentioned in Fig. 8. η_d is maximum during the start of the drying process because the surface and free moistures are removed when drying begins. It decreased with drying time from morning to evening. The maximum η_d was 78% and 46.9% during tomato and brinjal drying, respectively.

The average values of I_c and Q_a during the drying of tomato and brinjal are mentioned in Table 4. The thermal efficiency

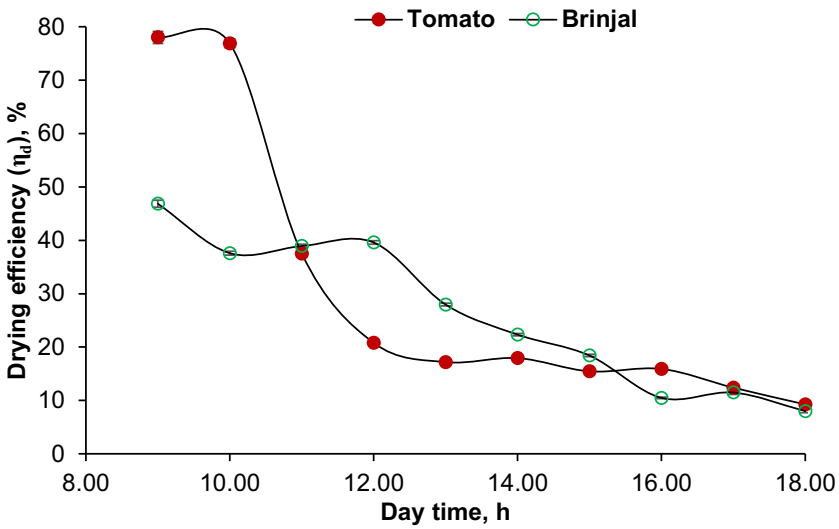

Fig. 8 Variations in drying efficiency (η_d) of ITSD with time

Table 4 Average measured data and performance of the ITSD

Material	day	Working time	Average radiation (I_c), W/m^2	Average Heat available for drying (Q_a), W	Average thermal efficiency SAC (η_c) %	Average dryer efficiency of the ITSD, (η_d) %	Solar fraction (SF)
Tomato	16th April 2018	8:00–18:00	753.14	824.46	59.05	31.4	1.89
Brinjal	1st April 2018	8:00–18:00	807.14	844.98	58.42	25.16	2.15

of SAC (η_c) and drying efficiency of ITSD (η_d) were estimated using Eqs. (5) and (9), respectively, and they are also mentioned in Table 4. It is found that the average η_c was 60.05% and 58.10% for tomato and brinjal, respectively. The average η_d was 31.40% and 25.16% for tomato and brinjal, respectively.

Also, the velocity of the air at collector inlet was measured throughout the day from 8.00 AM (mentioned as 0 min in X-axis) to 6.00 PM (mentioned as 120 min in X- axis) at each 5 min interval and it is mentioned in Fig. 9. It fluctuated continuously during the tomato drying experiments with a minimum, maximum and average velocity of 0.01 m/s, 2.45 m/s and 0.63 m/s, respectively, and for brinjal drying, they were 0.01 m/s, 2.78 m/s and 0.69 m/s, respectively. The thermal performance of ITSD has been evaluated with the help of a mass flow rate based on the average air velocity at the collector inlet.

3.2 Drying characteristic of tomato and brinjal

In this section, the results of tomato and brinjal slices during drying are analyzed. Fig. 10 shows the variation of MC of tomato as a function of drying time at different trays. From Fig. 10, it is observed that at a constant time, MC is decreased when the tray numbers moved from 1 to 4 because of the position of trays. The moisture removal rate is higher for the tray at bottom (tray – 1) as the slices face direct exposure to hot air from SAC. Trays – 2, 3 and 4 are placed above the tray – 1, therefore moisture removal rate is lower compared to tray – 1. The MC of tomato slices reduced from MC_i of 15.6667 kg/kg of db to MC_f of 0.4183, 0.5844, 0.8471, 1.3624 and 1.8583 kg/kg of db, at trays - 1, 2, 3, and 4 and OSD drying, respectively.

Tomato slices were dried in open sun drying (OSD) method and the results are also plotted in Fig. 10. As the drying chamber temperature is more than that of the T_{atm}, the moisture removal rate is higher for the material inside the drying cabinet than that of material in OSD. The final MC of tomato slices in tray – 1 is 0.4183 kg/kg of db: at the same time, during OSD drying, it is 1.8583 kg/kg of db, which is 344% higher in tray – 1 compared to OSD method. It is observed that the dried tomato slices from ITSD were clean with natural color and the slices in the OSD method were dusty and pale color.

Drying curves of brinjal were drawn from the measured data and they are shown in Fig. 11. MC of brinjal slices was reduced from MC_i of 10.111 kg/kg of db to MC_f of 0.3225, 0.3915, 0.57759, 0.7010, and 1.0793 kg/kg of db at trays - 1, 2, 3 and 4, and OSD drying, respectively. It is also observed that the natural color was retained in brinjal during ITSD drying and the color slightly faded in OSD drying because of dust in the open air.

Figure 12 gives the variation of average drying rate (DR_{av}) of tomato and brinjal slices with respect to time. DR is

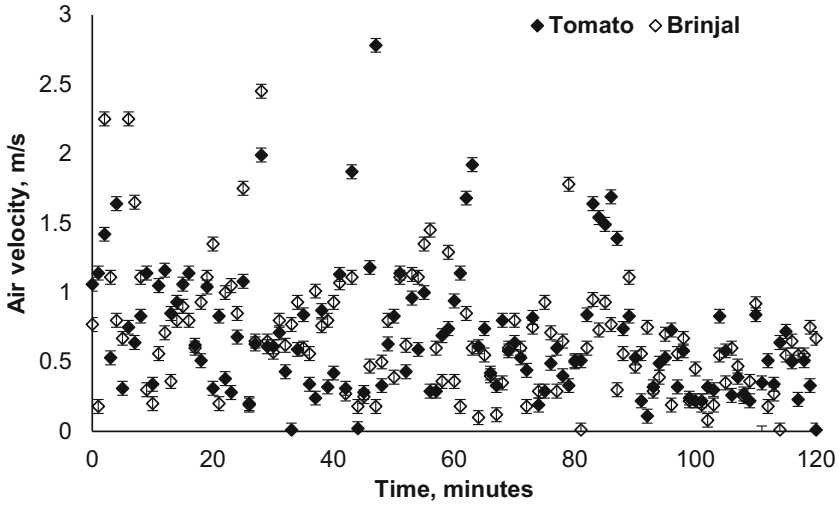

Fig. 9 Variation of velocity of the air at SAC inlet with respect to time

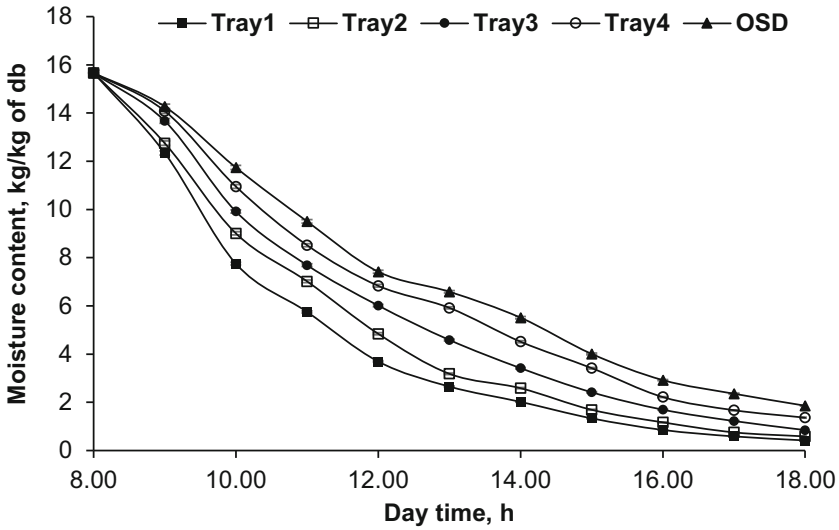

Fig. 10 Drying curve during tomato drying

estimated using Eq. (8). DR increased initially and then gradually decreased when drying time increased for both tomato and brinjal. The surface MC is removed during the start of drying therefore, DR is increased and is more during commencement. Once the surface MC is removed, maximum energy is needed to migrate interior MC to surfaces and it reduces DR which is one of the reasons for the decrease of DR during final time zones. Case hardening effect [31] is also one of the reasons for lower DR of food at the final time zone. From Fig. 12, it is also observed that the drying behavior of tomato is more than that of brinjal. Initial MC of tomato is higher than that of brinjal, therefore the drying rate (or moisture removal rate) is higher for tomato. Similarly, the drying rate variation of tomato and brinjal with moisture content (db) is presented in Fig. 13. The result of Fig. 12 is almost replicated in Fig. 13. The drying rates are higher in high MC regions for both cases. The drying rates are high (in high MC region) in tomato compared to brinjal because of the higher initial MC of tomato as already explained in Fig. 12.

Figure 14 shows the comparison of MR of tomato slices with existing empirical correlations. In X – axis, time 0 h indicates the starting drying time of 8.00 AM and 10 h indicates the end of drying time at 6.00 PM. For selecting a suitable model for drying kinetics of tomato slices, the present drying curves in the form of MR are fitted with four different available models given in Table 3. The model coefficients and constants for all the models mentioned in Table 3 are estimated and are given in Table 5. It is observed that the Page model [31] gives a higher correlation coefficient ($R^2 = 0.9986$) and lower reduced $\chi^2 = 0.00016$, which indicates a good fit compared to other models. Hence Page model [31] is considered as the best fitting model for tomato drying in ITSD. Also, the Wang and Singh [31] model and Henderson and Pabis [31] models give second and third highest R^2 of 0.9955 and

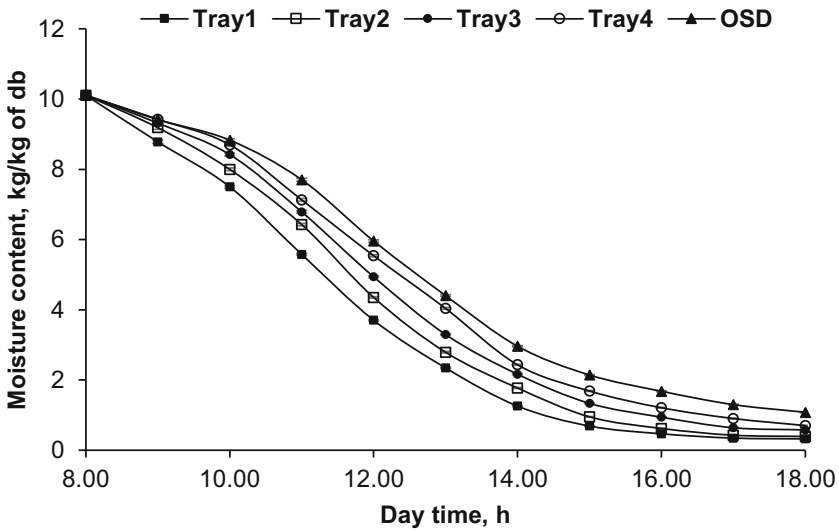

Fig. 11 Variation of MC during drying of brinjal

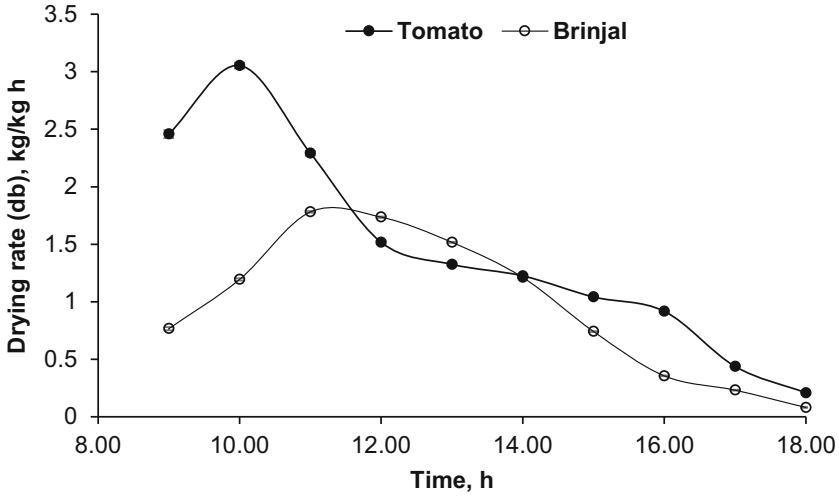

Fig. 12 Variation in drying rate of tomato and brinjal

0.9941, respectively hence they can also be used for tomato drying.

Similarly, experimental MR data of brinjal is fitted with various models. The correlation coefficients and constants are mentioned in Table 6. It is found that the drying model suggested by Page model [31] gives higher R^2 (0.9982) (Table 6) and lower χ^2 (0.00032**)** which indicates a good fit compared to other models (Fig. 15). The second best fit is noticed with Wang and Singh [31] model with R^2 of 0.9804.

The thermal performance of ITSD is compared with data in the existing literature and is shown in Table 7. In both tomato and brinjal drying processes, the present results with ITSD show better thermal performances (η_c and η_d) than the results of other studies. The temperature available at the collector outlet is more (in the range of 38 to 72 °C) due to higher radiation and V-shaped corrugated absorber plate which enhances the heat transfer rate.

3.3 Effective moisture diffusivity (D_{eff})

The temperature of the drying air varies with solar radiation which affects the drying behavior of the sample. Figure 16 shows the variation of D_{eff} with time. D_{eff} is estimated from Fick's diffusion model (Eq. 16). D_{eff} of tomato varies from 2.2859×10^{-9} to 6.0399×10^{-9} m^2/s with an average of 3.60×10^{-9} m^2/s while that of the brinjal varies from 2.2859×10^{-9} and 6.0324×10^{-9} m^2/s with an average of 4.00×10^{-9} m^2/s. D_{eff} of various food material was reported in Zogzas et al. [40] and they were in the range of 10^{-8} and 10^{-12} m^2/s, the obtained results from the present analysis are also in the same range. From Fig. 16, it is observed that D_{eff} increases with time for both tomato and brinjal. But the variation of D_{eff} in case of tomato and brinjal is almost linear. In the case of brinjal, D_{eff} increase is very steep up to 2.00 PM because of higher temperature of the product and after 2.00 PM, the steepness decreases because of decrease in solar radiation.

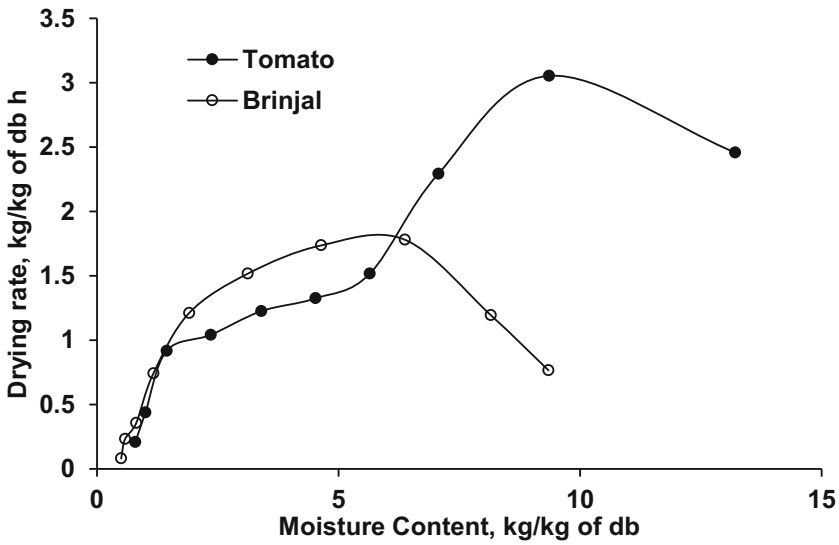

Fig. 13 Variation of drying rate with moisture content

Table 5 Statistical results for the various thin layer model available for Tomato (*Solanum lycopersicum*)

Model	Tray	Model coefficients	R^2	χ^2
Lewis or Newton [31]	Tray1	k = 0.3368	0.9921	0.00076
	Tray2	k = 0.0292	0.9920	0.00087
	Tray3	k = 0.2475	0.9912	0.00134
	Tray4	k = 0.2094	0.9841	0.00160
	OSD	k = 0.1821	0.9797	0.00191
Page model [31]	Tray1	k = 0.2870; n = 1.1264	0.9962	0.00041
	Tray2	**k = 0.2290; n = 1.1759**	**0.9986**	**0.00016**
	Tray3	k = 0.1805; n = 1.2093	0.9975	0.00029
	Tray4	k = 0.1463; n = 1.2226	0.9962	0.00043
	OSD	k = 0.1188; n = 1.2541	0.9955	0.00047
Henderson and Pabis [31]	Tray1	k = 0.3465; a = 1.0302	0.9941	0.00071
	Tray2	k = 0.3031; a = 1.0384	0.9940	0.00072
	Tray3	k = 0.2601; a = 1.0509	0.9912	0.00104
	Tray4	k = 0.2216; a = 1.0544	0.9890	0.00123
	OSD	k = 0.1188; a = 1.0587	0.9862	0.00144
Wang and Singh [31]	Tray1	a = −0.2412; b = 0.0149	0.9848	0.00182
	Tray2	a = −0.2186; b = 0.0125	0.9953	0.00057
	Tray3	a = −0.1904; b = 0.0097	0.9955	0.00083
	Tray4	a = −0.1640; b = 0.0072	0.9948	0.00058
	OSD	a = −0.1431; b = 0.0054	0.9938	0.00065
Two Term [31]	Tray1	k = 0.3465; g = 0.3465; a = 0.5151; b = 0.5151	0.9940	0.00094
	Tray2	k = 0.3031; g = 0.3030; a = 0.5192; b = 0.5192	0.9939	0.00092
	Tray3	k = 0.2601; g = 0.2601; a = 0.5255; b = 0.5255	0.9912	0.00134
	Tray4	k = 0.2216; g = 0.2216; a = 0.5272; b = 0.5272	0.9890	0.00158
	OSD	k = 0.1943; g = 0.19431; a = 0.5299; b = 0.5299	0.9863	0.00186

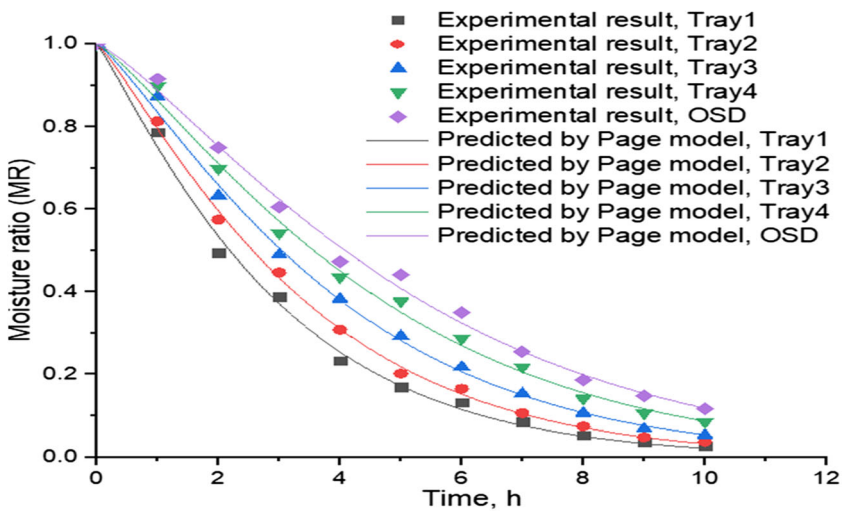

Fig. 14 Comparison of drying curve of tomato with Page model [31]

Table 6 Statistical results for the various thin layer models available for and Brinjal (*Solanum melongena*)

Model	Tray	Model coefficients	R^2	χ^2
Lewis or Newton [31]	Tray1	k = 0.2599	0.9405	0.00800
	Tray2	k = 0.2310	0.9220	0.01082
	Tray3	k = 0.2099	0.9203	0.01063
	Tray4	k = 0.1918	0.9140	0.01114
	OSD	k = 0.1792	0.9045	0.01211
Page model [31]	Tray1	k = 0.0906; *n* = 1.7233	0.9969	0.00046
	Tray2	k = 0.0611; *n* = 1.8684	0.9976	0.00037
	Tray3	**k = 0.0657; *n* = 1.8633**	**0.9982**	**0.00032**
	Tray4	k = 0.0468; *n* = 1.8554	0.9973	0.00039
	OSD	k = 0.0401; *n* = 1.8920	0.9944	0.00076
Henderson and Pabis [31]	Tray1	k = 0.2842; a = 1.1041	0.9532	0.00699
	Tray2	k = 0.2577; a = 1.1258	0.9409	0.00910
	Tray3	k = 0.2359; a = 1.1280	0.9414	0.08690
	Tray4	k = 0.2171; a = 1.1300	0.9375	0.00900
	OSD	k = 0.2044; a = 1.1339	0.9306	0.00979
Wang and Singh [31]	Tray1	a = −0.1871; b = 0.0084	0.9804	0.00220
	Tray2	a = −0.1598; b = 0.0054	0.9727	0.00323
	Tray3	a = −0.1415; b = 0.0036	0.9756	0.00276
	Tray4	a = −0.1233; b = 0.0018	0.9764	0.00259
	OSD	a = −0.1111; b = 0.0006	0.9766	0.00253
Two Term [31]	Tray1	k = 0.2842; g = 0.2842; a = 0.5521; b = 0.5521	0.9532	0.00899
	Tray2	k = 0.2578; g = 0.2578; a = 0.5629; b = 0.5629	0.9409	0.01171
	Tray3	k = 0.2359; g = 0.2359; a = 0.5638; b = 0.5638	0.9414	0.01117
	Tray4	k = 0.2171; g = 0.2171; a = 0.5651; b = 0.5651	0.9375	0.01157
	OSD	k = 0.20444; g = 0.20444; a = 0.56697; b = 0.56697	0.93058	0.01259

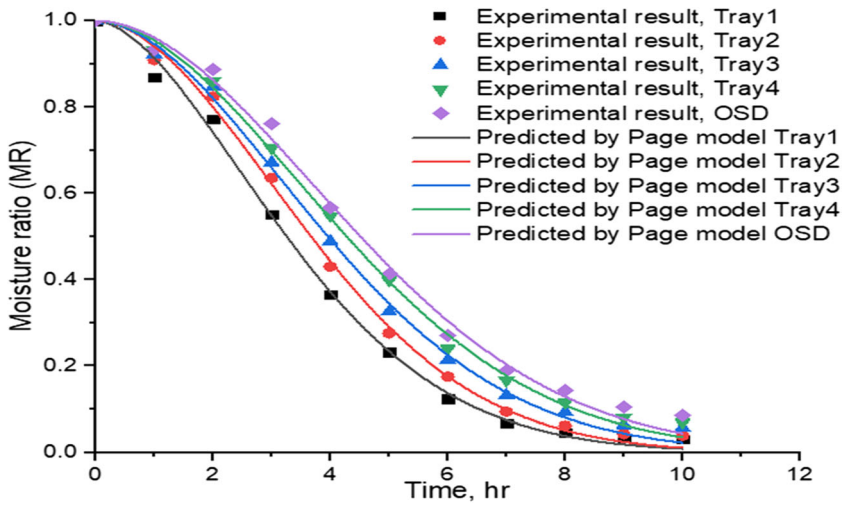

Fig. 15 Comparison of drying curve of brinjal slices with predicted model

Table 7 Estimated collector and dryer efficiency of this present analysis and comparison of same with existing studies

Dryer type	Product	Mass (kg)	Drying air temperature, °C	Drying Time, h	Average η_c, %	Average η_d, %
Present study ITSD with V-shape corrugated absorber	Tomato Brinjal	2 2	43–70 38–72	10 10	59.05% 58.42%	31.4% 25.16%
ITSD with sensible heat storage [37]	Bitter gourd	4	40–50	7	22%	19%
ITSD (forced convection type) [38]	Banana	1.5	33–45	16	38.21%	5.75%
ITSD with Double pass collector [39]	Red chili	40	32–67	33	28%	13%

3.4 Heat and mass transfer coefficients and activation energy

h_m for tomato and brinjal were estimated using Eqs. (16) and (17) and this was used to calculate h. Figs. 17 and 18 show h and h_m with drying time. From Figs. 17 and 18, it is observed that the variation of h and h_m is almost similar nature as both are simultaneous parameters.

The values of h_m are in the range of 1.86×10^{-4} to 3.33×10^{-3} m/s (with an average of 1.57×10^{-3} m/s) during tomato drying and 1.11×10^{-4} to 3.32×10^{-3} m/s with an average of 1.5×10^{-3} m/s for brinjal drying (Fig. 17). The values of h were in the range of 0.1886 to 3.3685 W/m^2 K during tomato drying and 0.1066 to 3.3564 W/m^2 K during brinjal drying (Fig. 18). Average h of tomato is 1.5879 W/m^{2}K and the same for brinjal is 1.5215 W/m^{2}K. Average h of 8.19 W/m^{2}K was reported in the numerical work of Chandramohan and Talukdar [41]'s convective drying of potato with air velocity of 0.1 to 0.3 m/s. The values are quiet low in this present analysis because it's a natural convection application. Lemus-Mondaca et al. [42]'s h variation is in the range of 0.25 to 4.55 W/m^{2}K for drying experiments with papaya slices. h_m values measured for a soil surface were in the range of 5 to 25×10^{-3} m/s [43]. h and h_m vary because of variation in MR with drying time. The curves of h and h_m (Figs. 17 and 18) report steep slopes up to 2.00 PM and thereafter, it becomes low because of slower drying rate.

Experimental results of h and h_m are used to generate correlations and they are;

For tomato,

$$h_m = 2 \times 10^{-7} t^3 - 03 \times 10^{-6} t^2 + 0.0003t - 0.0025, \quad (R2 = 0.998) \tag{20}$$

$$h = 0.0002t^3 - 0.0029t^2 + 0.3184t - 2.5623, \quad (R2 = 0.9989) \tag{21}$$

For Brinjal,

$$h_m = -8 \times 10^{-6} t^3 + 0.0003t^2 - 0.0041t + 0.0159, \quad (R2 = 0.9985) \tag{22}$$

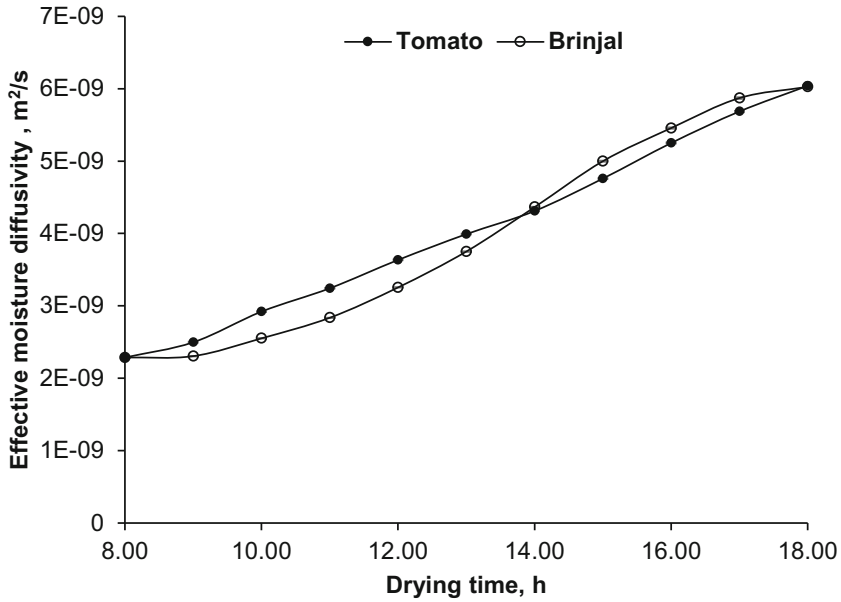

Fig. 16 Variation of D_{eff} with respect to drying time

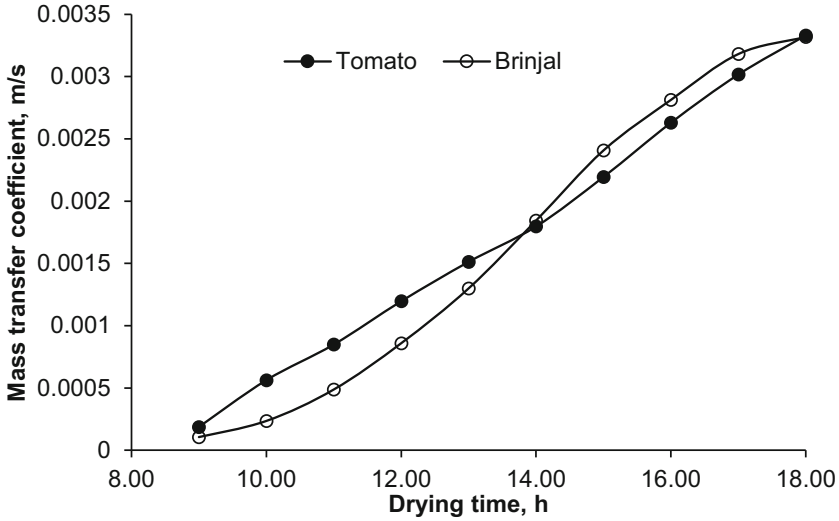

Fig. 17 Variation of mass transfer coefficient during drying in ITSD with time

$$h = -0.0083t^3 + 0.3423t^2 - 4.1808t + 16.077\ , \quad (\mathrm{R2} = 0.9985) \tag{23}$$

Figures 19 and 20 show the variation of h_m and h with MR of tomato and brinjal. From Fig. 19, it is observed that h_m increases with decrease of MR. h_m increases when MR is decreased which implies that the product loses its MC gradually. It is noticed that there is a steep increase of h_m at low MR region because of huge moisture transaction from the material. A similar analysis was performed for h variation with MR, but the nature of curve is same (Fig. 20).

Correlations were developed for h_m and h, these being:

$$\text{For tomato, } hm = -1 \times 10{-}3\ ln\ (\mathrm{MR}){-}9 \times 10{-}6, \quad (\mathrm{R2} = 1) \tag{24}$$

$$h = -1.136\ ln\ (\mathrm{MR}){-}0.009, \quad (\mathrm{R2} = 1) \tag{25}$$

$$\text{For brinjal, } hm = -1 \times 10{-}3\ ln\ (\mathrm{MR}){-}4 \times 10{-}6, \quad (\mathrm{R2} = 0.9999) \tag{26}$$

$$h = -1.123\ ln\ (\mathrm{MR}){-}0.0044, \quad (\mathrm{R2} = 1) \tag{27}$$

The activation energy (E) is evaluated by plotting the graph between $ln\ (D_{eff})$ and the inverse of the temperature [1/(T+ 273.15)] and is shown in Fig. 21. The temperature of drying air varies continuously during the experiments, so to find E, the instantaneous temperature values at each tray are considered as the temperature decreases from bottom tray to top tray (Tray 1 to 4). So E is calculated by considering the relation between $ln\ (D_{eff})$ and [1/ (T+ 273.15)] which gives the best fitting linear curve. The results obtained for E and D_o are shown in Table 8. From Table 8, it is observed that E is

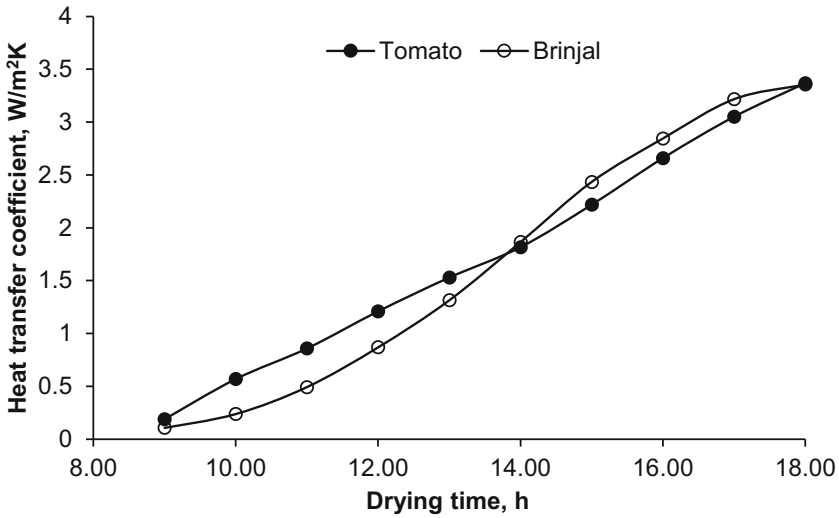

Fig. 18 Variation of heat transfer coefficient during drying in ITSD with time

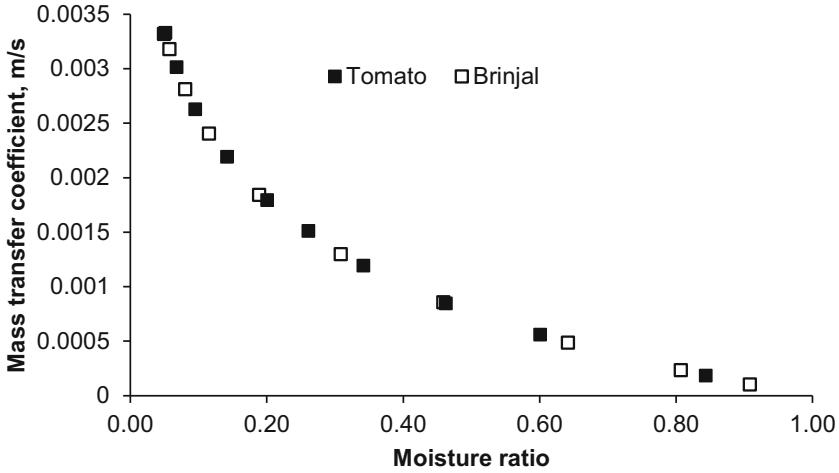

Fig. 19 Variation of mass transfer coefficient with moisture ratio during indirect solar drying

21.19 kJ/mol for tomato and 19.46 kJ/mol for brinjal. Doymaz [30] conducted experiments with tomatoes and found that E was in the range of 17.4 to 32.9 kJ/mol. Also, from this experimental analysis, it is found that the pre-exponential factors (D_o) for tomato and brinjal were 1.097×10^{-5} m^2/s and 6.37×10^{-6} m^2/s.

3.5 Experimental uncertainty analysis

The velocity of drying air, temperature and RH of the drying air were measured with Tenmar-Hot wire anemometer with probes. Mass of the sample was measured by OHAUS electronic weighing balance. Uncertainty values of the experimental parameters (Y) were calculated and are shown in Table 9. For a given calculated value of parameters Y, the uncertainty Z is determined by the root-sum square expression as given below:

$$Z = \left[\left(\frac{\partial Y}{\partial X_1}X_1\right)^2 + \left(\frac{\partial Y}{\partial X_2}X_2\right)^2 + \left(\frac{\partial Y}{\partial X_3}X_3\right)^2 + \ldots\ldots + \left(\frac{\partial Y}{\partial X_n}X_n\right)^2\right]^{1/2}, \tag{28}$$

Where X_n is uncertainty is the uncertainty in each measured variable.

4 Conclusions

An indirect type solar dryer (ITSD) was developed with a V-shaped absorber plate SAC for the drying of Tomato (*Solanum lycopersicum*) and Brinjal or eggplant (*Solanum melongena*). Drying experiments were performed and the drying kinetics of tomato and brinjal have been investigated. The

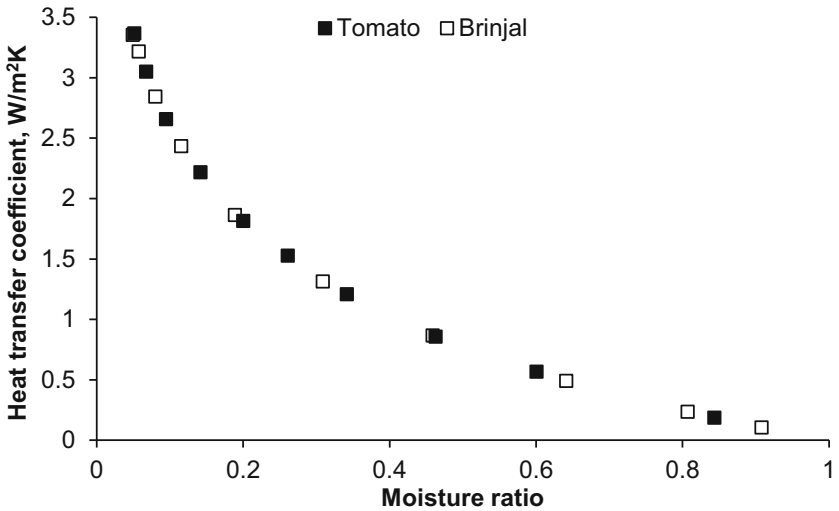

Fig. 20 Variation of heat transfer coefficient with moisture ratio during indirect solar drying

Table 8 Activation energy (E) and pre-exponential factor (D_o) for tomato and brinjal

Material	Activation Energy, (E), kJ/mol	Arrhenius factor (D_o) × 10^{-6} m/s	R^2
Tomato	21.19 ± 0.11	1.097×10^{-5}	0.9954
Brinjal	19.46 ± 0.10	6.30×10^{-6}	0.9978

temperature inside the drying chambers decreased when the hot air moved in an upward direction as the food products absorbed heat energy in each tray. The average temperature available at the collector outlet was 56.45 °C and 57.27 °C during tomato and brinjal drying, respectively. MC of the tomato and brinjal were reduced from 15.667 to 0.8028 kg/kg of db and from 10.111 to 0.4982 kg/kg of db, respectively. Page model followed by Wang and Singh model and Henderson and Pabis models were the best drying models for ITSD of tomato drying and the Page model followed by Wang and Singh model were the best drying models for brinjal drying. Average D_{eff} for tomato and brinjal were 3.60×10^{-9} m^2/s and 4.00×10^{-9} m^2/s, respectively. Mass transfer coefficient (h_m) was in the range of 0.82×10^{-4} to 2.85×10^{-3} m/s for tomato drying and 1.11×10^{-4} to 3.32×10^{-3} m/s. Heat transfer coefficient (h) was in the range of 0.0892 to 2.888 and 0.1066 to 3.3564 W/m^2 K for tomato and brinjal drying, respectively. h_m and h correlations were developed in terms of drying time and DR. Activation energy was 21.19 and 19.46 kJ/mol for tomato and brinjal, respectively. The drying efficiency of the system was 31.4% and 25.16% and the average thermal efficiency of the SAC was 59.05%and 58.42% during tomato and brinjal drying, respectively. The system performance of the developed ITSD was higher compared to data available in the literature because a higher temperature range (38 to 72 °C) was achieved inside the drying chamber.

Table 9 Uncertainties of the parameters during drying experiments

Parameters	Uncertainty
Temperature	±1 °C
Relative humidity (RH)	±2%
Air inlet velocity	±0.03 m/s
Solar radiation	± 10 W/m^2
Mass	± 0.0002 g
Moisture content, tomato	0.027 kg per kg of db
Moisture content, brinjal	0.012 kg per kg of db
Moisture ratio, tomato	0.025
Moisture ratio, brinjal	0.014
Actual heat supplied, tomato	± 25.24 W
Actual heat supplied, brinjal	± 25.40 W
Moisture diffusivity, tomato	0.31%
Moisture diffusivity, brinjal	0.21%
Heat transfer coefficient, tomato	± 0.011 W/m^2K
Heat transfer coefficient, brinjal	± 0.012 W/m^2K
Mass transfer coefficient, tomato	1.08×10^{-5} m/s
Mass transfer coefficient, brinjal	1.18×10^{-5} m/s
Activation energy, tomato	± 0.11 kJ/mol
Activation energy, brinjal	± 0.10 kJ/mol
Drying efficiency, tomato	± 1.13%,
Drying efficiency, brinjal	± 0.65%,

Acknowledgements The authors would like to thank Department of Mechanical Engineering, National Institute of Technology Warangal, India for funding this project. The project approval number is: NITW/MED/Head/2015/408.

The author acknowledges with thanks the support received by way of proof reading from Dr. M. R. Vishwanathan, Assistant Professor of English, Head, Humanities and Social Science Department, NIT Warangal, India.

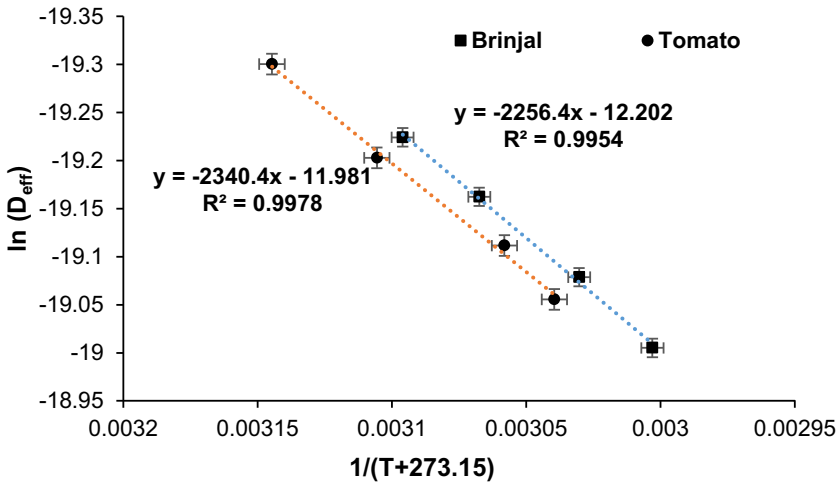

Fig. 21 Arrhenius-type relationship between D_{eff} and temperature for tomato and brinjal

Compliance with ethical standards

Conflict of interest On behalf of all authors, the corresponding author states that there is no conflict of interest.

References

1. Jha SN, Vishwakarma RK, Ahmad T, Rai A, Dixit AK (2015) Report on Assesment of Quantitive harvest and post-harvest losses of major crops and Commodities in India, Ministry of Food Processing Industries (Govt. of India), ICAR-CIPHET, PO: PAU, Ludhiana-141004, India
2. Husham Abdulmalek S, Khalaji Assadi M, Al-Kayiem HH, Gitan AA (2018) A comparative analysis on the uniformity enhancement methods of solar thermal drying. Energy 148:1103–1115. https://doi.org/10.1016/j.energy.2018.01.060
3. Yadav S, Chandramohan VP, Lingayat AB et al (2018) Numerical analysis on thermal energy storage device with finned copper tube for an indirect type solar drying system. J Sol Energy Eng 140:1–13. https://doi.org/10.1007/s00231-018-2390-7
4. Patel SS, Lanjewar A (2019) Performance study of solar air heater duct with gap in V-rib with symmetrical gap and staggered ribs. Heat Mass Transf 1–16|. https://doi.org/10.1007/s00231-019-02592-3
5. Arunachalam U, Edwin M (2017) Experimental investigations on thermal performance of solar air heater with different absorber plates. Heat Mass Transf 35:393–397. https://doi.org/10.18280/ijht.350223
6. Darici S, Kilic A (2020) Comparative study on the performances of solar air collectors with trapezoidal corrugated and flat absorber plates. Heat Mass Transf 56:1833–1843. https://doi.org/10.1007/s00231-020-02815-y
7. Ringeisen B, Barrett DM, Stroeve P (2014) Concentrated solar drying of tomatoes. Energy Sustain Dev 19:47–55. https://doi.org/10.1016/j.esd.2013.11.006
8. Atalay H (2019) Performance analysis of a solar dryer integrated with the packed bed thermal energy storage (TES) system. Energy 172:1037–1052. https://doi.org/10.1016/j.energy.2019.02.023
9. Oberoi SPD, Sogi DS (2015) Drying kinetics, moisture diffusivity and lycopene retention of watermelon pomace in different dryers. J Food Sience Technol 52:7377–7384. https://doi.org/10.1007/s13197-015-1863-7
10. Monteiro RL, Link JV, Tribuzi G, Carcio BAM (2018) Microwave vacuum drying and multi- flash drying of pumpkin slices. J Food Eng 232:1–10. https://doi.org/10.1016/j.jfoodeng.2018.03.015
11. Torki-Harchegani M, Ghasemi-Varnamkhasti M, Ghanbarian D et al (2016) Dehydration characteristics and mathematical modelling of lemon slices drying undergoing oven treatment. Heat Mass Transf 52:281–289. https://doi.org/10.1007/s00231-015-1546-y
12. Akpinar EK, Bicer Y (2005) Modelling of the drying of eggplants in thin-layers. Int J Food Sci Technol 40:273–281. https://doi.org/10.1111/j.1365-2621.2004.00886.x
13. Doymaz I, Göl E (2011) Convective drying characteristics of eggplant slices. J Food Process Eng 34:1234–1252. https://doi.org/10.1111/j.1745-4530.2009.00426.x
14. El-Sebaii AA, Shalaby SM (2013) Experimental investigation of an indirect-mode forced convection solar dryer for drying thymus and mint. Energy Convers Manag 74:109–116. https://doi.org/10.1016/j.enconman.2013.05.006
15. Dissa AO, Bathiebo DJ, Desmorieux H et al (2011) Experimental characterisation and modelling of thin layer direct solar drying of Amelie and brooks mangoes. Energy 36:2517–2527. https://doi.org/10.1016/j.energy.2011.01.044
16. Wilkins R, Brusey J, Gaura E (2018) Modelling uncontrolled solar drying of mango waste. J Food Eng 237:44–51. https://doi.org/10.1016/j.jfoodeng.2018.05.012.This
17. Wang W, Li M, Hassanien R et al (2018) Thermal performance of indirect forced convection solar dryer and kinetics analysis of mango. Appl Therm Eng 134:310–321. https://doi.org/10.1016/j.applthermaleng.2018.01.115
18. Shrivastava V, Kumar A (2016) Experimental investigation on the comparison of fenugreek drying in an indirect solar dryer and under open sun. Heat Mass Transf 52:1963–1972. https://doi.org/10.1007/s00231-015-1721-1
19. Kavak Akpinar E (2019) The effects of some exergetic indicators on the performance of thin layer drying process of long green pepper in a solar dryer. Heat Mass Transf 55:299–308. https://doi.org/10.1007/s00231-018-2415-2
20. Tiwari S, Tiwari GN (2018) Grapes (Vitis vinifera) drying by semi-transparent photovoltaic module (SPVM) integrated solar dryer: an experimental study. Heat Mass Transf 54:1637–1651. https://doi.org/10.1007/s00231-017-2257-3
21. Arunsandeep G, Lingayat A, Chandramohan VP et al (2018) A numerical model for drying of spherical object in an indirect type solar dryer and estimating the drying time at different moisture level and air temperature. Int J Green Energy 15:189–200. https://doi.org/10.1080/15435075.2018.1433181
22. Mahapatra A, Tripathy PP (2019) Experimental investigation and numerical modeling of heat transfer during solar drying of carrot slices. Heat Mass Transf und Stoffuebertragung 55:1287–1300. https://doi.org/10.1007/s00231-018-2492-2
23. Naik R, Arunsandeep G, Chandramohan VP (2017) Numerical simulation for freeze drying of skimmed Milk with moving sublimation front using tri-diagonal matrix algorithm. J Appl Fluid Mech 10:813–818. https://doi.org/10.18869/acadpub.jafm.73.240.27054
24. Godireddy A, Lingayat A, Naik RK et al (2017) Numerical solution and it's analysis during solar drying of green peas. J Inst Eng Ser C 99:571–579. https://doi.org/10.1007/s40032-017-0379-5
25. MNRE Indian Meteorological Department ND (India) (2008) Solar radiation hand book, Solar Energy Centre
26. Balijepalli R, Chandramohan VP, Kirankumar K (2017) Performance parameter evaluation , materials selection , solar radiation with energy losses , energy storage and turbine design procedure for a pilot scale solar updraft tower. Energy Convers Manag 150:451–462. https://doi.org/10.1016/j.enconman.2017.08.043
27. Abhay L, Chandramohan VP, Raju VRK (2018) Numerical analysis on solar air collector provided with artificial square shaped roughness for indirect type solar dryer. J Clean Prod 190:353–367. https://doi.org/10.1016/j.jclepro.2018.04.130
28. Chandramohan VP (2016) Numerical prediction and analysis of surface transfer coefficients on moist object during heat and mass transfer application. Heat Transf Eng 37:53–63. https://doi.org/10.1080/01457632.2015.1042341
29. Nguyen M, Price WE (2007) Air-drying of banana : Influence of experimental parameters , slab thickness , banana maturity and harvesting season. J Food Eng 79:200–207. https://doi.org/10.1016/j.jfoodeng.2006.01.063
30. Doymaz I (2007) Air-drying characteristics of tomatoes. J Food Eng 78:1291–1297. https://doi.org/10.1016/j.jfoodeng.2005.12.047
31. Akpinar EK (2010) Drying of mint leaves in a solar dryer and under open sun: Modelling, performance analyses. Energy Convers Manag 51:2407–2418. https://doi.org/10.1016/j.enconman.2010.05.005
32. Doymaz I (2008) Convective drying kinetics of strawberry. Chem Eng Process Process Intensif 47:914–919. https://doi.org/10.1016/j.cep.2007.02.003

33. Crank J (1975) The mathematics of diffusion, (2nd ed.). Oxford University Press, London
34. Koua BK, Koffi PME, Gbaha P, Kamenan KB, Magloire Ekoun Koffi P, Gbaha P (2017) Evolution of shrinkage, real density, porosity, heat and mass transfer coefficients during indirect solar drying of cocoa beans. J Saudi Soc Agric Sci Accepted m:1–11. https://doi.org/10.1016/j.jssas.2017.01.002
35. Upadhyay A, Chandramohan VP (2016) Simultaneous heat and mass transfer model for convective drying of building material. J Inst Eng Ser C 99(2):239–245. https://doi.org/10.1007/s40032-016-0260-y
36. Cussler EL (2009) Diffusion: mass transfer in fluid systems, 3rd edn. Cambridge University Press, The Edinburg Building, Cambridge CB2 8RU, UK
37. Vijayan S, Arjunan TV, Kumar A (2016) Mathematical modeling and performance analysis of thin layer drying of bitter gourd in sensible storage based indirect solar dryer. Innov Food Sci Emerg Technol 36:59–67. https://doi.org/10.1016/j.ifset.2016.05.014
38. Hegde VN, Hosur VS, Rathod SK et al (2015) Design, fabrication and performance evaluation of solar dryer for banana. Energy Sustain Soc 5:2–12. https://doi.org/10.1186/s13705-015-0052-x
39. Fudholi A, Sopian K, Yazdi MH et al (2014) Performance analysis of solar drying system for red chili. Sol Energy 99:47–54. https://doi.org/10.1016/j.solener.2013.10.019
40. Zogzas NP, Maroulis ZB, Marinos-Kouris D (2007) Drying technology : an international journal moisture diffusivity data compilation in foodstuffs. Dry Technol:37–41. https://doi.org/10.1080/07373930701438592
41. Chandramohan VP, Talukdar P (2010) Three dimensional numerical modeling of simultaneous heat and moisture transfer in a moist object subjected to convective drying. Int J Heat Mass Transf 53:4638–4650. https://doi.org/10.1016/j.ijheatmasstransfer.2010.06.029
42. Lemus-Mondaca RA, Zambra CE, Vega-Gálvez A, Moraga NO (2013) Coupled 3D heat and mass transfer model for numerical analysis of drying process in papaya slices. J Food Eng 116:109–117. https://doi.org/10.1016/j.jfoodeng.2012.10.050
43. Sauer TJ, Norman JM, Tanner CB, Wilson TB (1995) Measurement of heat and vapor transfer coefficients at the soil surface beneath a maize canopy using source plates. Agric For Meteorol 75:161–189. https://doi.org/10.1016/0168-1923(94)02209-3